Published in final edited form as:
Clin Cancer Res. 2009 May 15; 15(10): 3256–3264. doi:10.1158/1078-0432.CCR-08-2661.

Adiponectin-deficiency limits tumor vascularization in the MMTV-PyV-mT mouse model of mammary cancer

Martin S. Denzel[1], **Lionel W. Hebbard**[1], **Gregory Shostak**[2], **Lawrence Shapiro**[2], **Robert D. Cardiff**[3], and **Barbara Ranscht**[1]

[1]Burnham Institute for Medical Research, La Jolla, California

[2]Eye Institute, Columbia University, New York, New York

[3]Center for Comparative Medicine and Pathology Department, University of California, Davis, Davis, California

Abstract

Purpose—High levels of the fat-secreted cytokine adiponectin are present in the circulation of healthy people while low levels correlate with an increased incidence of breast cancer in women. The current study experimentally probes the physiological functions of adiponectin in mammary cancer in a newly generated genetic mouse model.

Experimental Design—We established an adiponectin null mouse model of mammary cancer by introducing the polyoma virus middle T (PyV-mT) oncogene expressed from mouse mammary tumor virus (MMTV) regulatory elements into adiponectin null mice. MMTV-PyV-mT-induced tumors resemble ErbB2 amplified human breast cancers. We monitored tumor onset, kinetics and animal survival, and analyzed vascular coverage, apoptosis and hypoxia in sections from the primary tumors. Metastatic spreading was evaluated by analyses of the lungs.

Results—Adiponectin prominently localized to the vasculature in human and mouse mammary tumors. In adiponectin null mice, MMTV-PyV-mT-induced tumors appeared with delayed onset and exhibited reduced growth rates. Affected animals survived control tumor-bearing mice by an average of 21 days. Pathological analyses revealed reduced vascularization of adiponectin null tumors along with increased hypoxia and apoptosis. At experimental endpoint, adiponectin null transgenic mice showed increased frequency of pulmonary metastases.

Conclusion—The current work identifies a pro-angiogenic contribution of adiponectin in mammary cancer that in turn affects tumor progression. Adiponectin interactions with vascular receptors may be useful targets for developing therapies aimed at controlling tumor vascularization in cancer patients.

Correspondence: Barbara Ranscht, Burnham Institute for Medical Research, 10901 North Torrey Pines Road, La Jolla, CA 92037. Phone: 858-646-3122; Fax: 858-646-3197; E-mail: ranscht@burnham.org..

Statement of Translational Relevance

Adiponectin is an adipocyte-secreted cytokine that is abundant in the circulation. Clinical studies correlate low serum levels with obesity-related metabolic and vascular diseases and increased breast cancer incidence in women. To probe the functions of adiponectin in mammary tumorigenesis, we have generated and analyzed an adiponectin null mouse genetic model that mimics ErbB2-positive breast cancer in humans. Our studies identify a novel and unexpected pro-angiogenic contribution of adiponectin in tumor progression. We find adiponectin in association with the tumor vasculature while tumor cells are negative. The null mutation delays tumor onset, reduces tumor growth and prolongs life of affected animals over controls. Primary tumors in adiponectin null mice show reduced blood vessel infiltration along with increased hypoxia and apoptosis. Autopsies at experimental endpoint reveal increased pulmonary metastases. Our data provide evidence for a novel pro-angiogenic contribution of adiponectin to mammary cancer, and raise the possibility of exploring adiponectin-mediated vascular interactions as a target for cautious short-term and combination therapies of cancer patients.

Keywords

adiponectin; breast cancer; angiogenesis; hypoxia; metastasis

Introduction

The dependence of tumor growth and progression on the stromal microenvironment has inspired an intense body of research into the identification of factors that regulate these processes (1). While much of this work has concentrated on vascular factors and inflammatory responses, less is known about the role of adipocyte-derived signals on cancer progression. Adiponectin (also known as ACRP30, AdipoQ, and GBP28) is a circulating adipocytokine that is implicated in metabolic and vascular regulation. Serum levels are inversely correlated with obesity-related metabolic disorders, insulin resistance, hypertension, coronary heart disease and stroke (2-5). Clinical studies correlate low adiponectin levels in women with an increased risk of mammary cancer (6,7) and a metastatic tumor phenotype (8). These data have led to the suggestion that adiponectin exerts a cancer protective function. Indeed, adiponectin treatment reduces the proliferation of select human mammary cancer cell lines *in vitro* and *in vivo* (9). On the other hand, adiponectin affects the vasculature that critically supports tumor growth and progression by providing nutrients and oxygen (10). Adiponectin induces blood vessel infiltration into matrigel plaques (11), and regulates angiogenesis in the experimental hindlimb ischemia model (12). A similar pro-angiogenic role may play into tumor progression. Adiponectin-deficient mice develop normally until early adulthood and show no overt phenotype as judged by numerous physiological and metabolic parameters (12,13).

To distinguish the cellular functions of adiponectin in mammary cancer, we have generated an adiponectin null mouse genetic model that mimics human disease. Thirty percent of human breast cancers are characterized by overexpression of the receptor tyrosine kinase ErbB2 (14). The viral polyoma middle T (PyV-mT) oncogene is a membrane-associated surrogate for ErbB2 (Her2/neu) heterodimers (15). Transgenic PyV-mT expression through mouse mammary tumor virus (MMTV) regulatory elements leads to ligand-independent activation of mitogen-activated protein kinase (MAPK) and phosphatidylinositol 3-kinase (PI3K) cascades in the mammary epithelium (15). The same signaling pathways are stimulated in Neu/ErbB2 transgenic murine mammary carcinomas and in human breast cancers overexpressing ErbB2 (14). Gene expression profiles show similarities of MMTV-PyV-mT-driven tumors to human luminal type B breast cancers (16). The PyV-mT model reiterates the stages of human carcinoma progression both by morphology and biomarker expression (17), including the loss of luminal marker Gata-3 (18-20). In humans, poor clinical outcome is linked to ErbB2 overexpression and loss of estrogen receptor (ER) gene expression (21-23), and similarly, advanced murine MMTV-PyV-mT-induced tumors display ErbB2 amplification and ER loss (17,24). Finally, MMTV-PyV-mT transgenic mice develop metastatic cancer mimicking the clinically advanced stage of human mammary carcinoma progression (25). We have used this clinically relevant breast cancer model to probe the functions of adiponectin in tumorigenesis. By generating and analyzing adiponectin null MMTV-PyV-mT transgenic mice, we reveal a novel and surprising contribution of adiponectin to mammary tumor vascularization. This phenotype mimics that of MMTV-PyV-mT mice lacking the adiponectin-binding protein T-cadherin (26) and implicates a functional link between these proteins in the crosstalk between tumor cells and the stromal microenvironment in mammary cancer.

Materials and Methods

Mice

C57Bl/6 adiponectin knock-out (APN-KO) mice were generated in Dr. Yuji Matsuzawa's laboratory (Osaka University, Osaka) (13). Dr. William Muller (McGill University, Montreal) first generated the MMTV-PyV-mT transgenic mice. For experiments reported in this study, we used mice with the MMTV-PyV-mT transgene in the C57Bl/6 background provided by Dr. Leslie Ellies (University of California San Diego). Generation of APN-KO MMTV-PyV-mT mice: MMTV-PyV-mT males were crossed with homozygous APN-KO females. The male APN-heterozygous MMTV-PyV-mT offspring was bred with APN-KO or WT females yielding MMTV-PyV-mT APN-WT and APN-KO females. Genotypes were determined by PCR. APNfor 5′-GGAACTTGTGCAGGTTGGAT-3′ and APNrev 5′-CAGTGCAAGCTCCAAGATGA-3′ amplified the WT 266-bp DNA fragment. APNKOfor 5′-ATACTTTCTCGGCAGGAGCA-3′ and APNrev amplified the 900 bp KO DNA fragment. We confirmed lack of adiponectin protein in APN-KO animals by ELISA (R&D) (Supplemental Table 1). Animals were fed with a normal diet.

Tumor formation and analysis

Tumor onset was monitored twice weekly by palpation. Tumor sizes were measured with digital calipers twice weekly and the volume was calculated as (length x width^2)/2. Animals were sacrificed when the tumor burden visibly affected the host or when the tumors reached the institutionally set limit of 20 mm along one axis. Statistical analysis of tumor onset and survival was done in Prism using log-rank test, and growth kinetics was analyzed using linear regression.

Immunoblotting

Mammary gland or tumor tissue was mechanically dissociated in lysis buffer (50 mmol/L Tris HCl pH 7.4, 150 mmol/L NaCl, 5 mmol/L EDTA, 1 mmol/L DTT, 1/100 protease inhibitor cocktail (Sigma), 0.1 mmol/L phenylmethylsulfonyl fluoride and 1% NP40). Protein (10 μg per lane) was separated by reducing SDS-PAGE and transferred to PVDF membranes. T-cadherin, adiponectin and β-tubulin were detected using specific antibodies and the ECL Detection Kit (Amersham).

Quantitative real-time PCR

Total RNA was extracted from normal mammary gland or tumor tissue using Trizol (Invitrogen). Equal amounts were reverse transcribed using oligo $(dT)_{18}$ and random hexamer primers (Transcriptor First Strand cDNA Synthesis Kit, Roche). Real-time PCR analysis was performed with SYBR green using the Stratagene Mx3000p instrument. T-cadherin (5′-catcgaagctcaagatatgg-3′; 5′-gatttccattgatgatggtg-3′), AdipoR1 (5′- acacagagactggcaacatc-3′; 5′- gagcaatccctgaatagtcc-3′), and AdipoR2 (5′- tggacacatctcctaggttg-3′; 5′-tagagaagagtcgggagacc-3′) cDNAs were detected and normalized to GAPDH (5′-ccagtatgactccactcacg-3′; 5′-gactccacgacatactcagc-3′).

Tissue preparation and histology

Tumors and lungs were fixed over night in 10% zinc formalin (Fisher), embedded in paraffin, then sectioned and stained with H&E. For pathologic evaluation, Dr. Cardiff examined 33 tumors from 17 WT mice and 16 tumors from 31 APN-KO mice as well as the lungs from 10 WT and 12 APN-KO mice. Snap-frozen fresh mammary glands were sectioned and fixed with ice-cold acetone.

Immunohistochemistry

Tumor sections were deparaffinized and incubated with 3% hydrogen peroxide in PBS. For CD31 staining, sections were digested with 0.1% trypsin (Zymed). For PCNA staining, sections were treated with target retrieval solution (DAKO). Endogenous biotin was blocked with avidin biotin kit (Vector labs). Sections were incubated with antibodies for CD31 (Pharmingen) or proliferating cell nuclear antigen (PCNA, Chemicon), and staining was detected with the respective biotinylated secondary IgGs (Pharmingen), streptavidin/horseradish peroxidase (Vector Labs ABC standard) and 3,3′-Diaminobenzidine (DAKO). CD31-labeled sections were counterstained with hematoxylin, and PCNA-stained sections with methyl green. Apoptotic cells were identified by the terminal deoxyribonucleotidyl transferase-mediated dUTP nick end label (TUNEL, Millipore). Hypoxic tumor areas were visualized using Hypoxyprobe™-1 Plus (Natural Pharmacia International). TUNEL and Hypoxyprobe™ stained sections were counterstained with methyl green.

Acetone-fixed mouse or human mammary gland sections were air dried and blocked in PBS containing 10% fetal calf serum (FCS), 1% bovine serum albumin (BSA) and 0.2% Triton X-100. Sections were then incubated with adiponectin (PA1-054, Affinity Bioreagents and R&D), CD31 (MEC 13.3, Pharmingen) and T-cadherin (26) antibodies. Alexa 488 and Alexa 594 fluorescent conjugates (Molecular Probes) were used to detect the respective primary antibodies. Negative controls were slides processed in parallel without primary antibody. For T-cadherin and adiponectin, tissues from KO animals were used as additional controls.

Mammary gland whole mounts

Mammary glands were processed as described previously (26).

Image acquisition and analysis

Whole mounts were digitized with an Epson Perfection 4490 Photo scanner and analyzed using ImagePro and Prism (unpaired t-test). Images of fluorescently stained mammary glands were acquired using a Fluoview 1000 confocal microscope (Olympus). For quantitative analyses, CD31, PCNA, TUNEL, Hypoxyprobe™ and H&E stained sections were scanned using the Aperio ScanScope XT® System (27) at 20x magnification (resolution of 0.5 um/pixel). This automated microscope generates high-resolution whole slide images of the full face of tissue sections and does not restrict analysis to representative images. The two largest tumors from each mouse were used for analyses; one section was analyzed from each tumor. Image analysis was performed using the web-based digital pathology information management software Aperio Spectrum® software (www.aperio.com). Number of lung metastases (foci of metastatic adenocarcinomas lodged in the lung parenchyma) was counted manually and blinded using at least five serial sections from each of the three lobes of the right lungs. CD31 and hypoxyprobe staining was quantified using a brown versus blue deconvolution algorithm yielding the ratio of positive signal area versus whole tumor area. An algorithm detecting the ratio of positive nuclei versus all nuclei in a complete tumor section was used for analysis of PCNA and TUNEL staining. Statistical analyses were performed in Prism using unpaired t-test or nonparametric Mann-Whitney test.

Corneal vascularization assay

Slow release hydron-pellets (Sigma) (0.4×0.4×0.2mm) contained 180 ng VEGF (R&D) or 500 ng high-molecular-weight adiponectin or PBS. Adult male WT mice were anesthetized with Avertin (0.015ml/g), and the pellet was implanted into the corneal stroma of one or both eyes at a distance of 2 mm from the corneo-scleral limbus. Clock hours of neovascularization (CN) and maximal vessel length (VL) were measured after 10 days, angiogenic area was calculated as 0.2 x π x VL (mm) x CN (mm) (28).

Generation of recombinant high molecular weight adiponectin

Adiponectin was isolated as described previously (29).

Results

Adiponectin Associates with the Mammary Gland Vasculature

Since little is known about the localization and cellular binding sites for adiponectin in the mouse mammary gland, we first examined adiponectin's distribution in normal tissue. Immunohistochemistry of fat pads from 60-day-old virgin females detected adiponectin in prominent association with blood vessels identified by endothelial cell marker CD31 expression (Fig. 1A). The vascular adiponectin signal was abolished in the fat pads from adiponectin null (APN-KO) mice (Fig. 1A) supporting the specificity of the antibody reagents. No overt differences in vascular density were noted between genotypes in the normal mammary gland. Vascular endothelial cells profusely express the adiponectin binding protein T-cadherin (26). To determine if adiponectin codistributes with GPI-linked T-cadherin on endothelial cell membranes, we performed double-labeling immunohistochemisty with goat anti-adiponectin and rabbit anti-T-cadherin antibodies (26). Adiponectin precisely mirrored the punctate pattern of T-cadherin on the capillaries in mammary fat pads (Fig. 1A, g-i). No specific adiponectin staining could be identified in the ductal epithelium (not shown). In order to validate the mouse model, we compared the distribution of T-cadherin and adiponectin in the human normal breast and in a mammary ductal invasive carcinoma biopsy. As in the mouse model, capillaries are positive for T-cadherin and adiponectin in human tissue (Supplementary Fig. 1). Together with our previous finding that the vascular adiponectin association depends on T-cadherin expression (26), these data demonstrate that the vasculature is a major site for adiponectin binding in the human and mouse mammary gland.

To address a possible contribution of adiponectin to mammary gland development, we compared the ductal patterning of whole mounted, carmine-stained mammary glands from virgin WT and APN-KO females at 21, 35, 56 and 84 days of age. Ductal growth and branching showed no apparent differences between genotypes (Supplementary Fig. 2). Moreover, APN-KO females nourished multiple normal size litters (data not shown). Thus, normal mammary gland development and function occur independent of adiponectin.

Adiponectin and Adiponectin-Receptor Expression in the MMTV-PyV-mT Mouse Mammary Tumor Model

Transgenic expression of PyV-mT from mouse mammary tumor virus promotor/enhancer elements (MMTV) produces tumors progressing from premalignant to malignant stages with distant metastases in all female mice (25). In MMTV-PyV-mT-induced neoplastic areas of mammary glands of 120-day-old mice and in tumors of 170 day old mice, adiponectin was specifically associated with the vasculature [unpublished data; (26)]. Since some breast cancers in women correlate with low adiponectin levels (6,7), we investigated if serum adiponectin levels show a similar decrease in the MMTV-PyV-mT model. ELISA analyses of serum from normal and tumor-bearing female mice at 85 and 150 days of age identified similar adiponectin concentrations in tumor-free (5.6 ± 0.11 μg/mL) and tumor-bearing (5.41 ± 0.31 μg/mL) animals (n = 6 per group; Supplementary Table 1). No serum adiponectin was detected in APN-KO mice. Thus, in the MMTV-PyV-mT model, tumor formation is not linked to reduced serum adiponectin concentrations.

To determine how adiponectin association in the mammary gland correlates with tumorigenesis, we compared adiponectin levels in the fat pads from normal and tumor-bearing mice by Western blotting. In transgenic MMTV-PyV-mT tumors from 150-day-old females, levels of adiponectin and the adiponectin-interacting protein T-cadherin were dramatically

reduced in comparison to normal virgin fat pads from 85-day-old mice (Fig. 1B). No adiponectin was detected in normal or tumor tissue from APN-KO mice (Fig. 1B). APN-KO PyV-mT tumors displayed reduced T-cadherin levels that were similar to that in the wild type transgenic condition.

In addition to T-cadherin, adiponectin interacts with the two seven-pass transmembrane adiponectin receptors 1 and 2 [AdipoR1 and AdipoR2; (30)]. To correlate expression levels of these receptors with tumor progression, we examined mRNA expression levels in normal and tumorigenic mammary glands by quantitative real-time PCR (Fig. 1C). T-cadherin mRNA was reduced in tumors compared to normal breast tissue confirming the protein expression data. In addition, mRNA levels for AdipoR2 were significantly diminished in PyV-mT tumors, while mRNA for AdipoR1 remained unchanged (Fig. 1C). These combined data suggest the coordinate reduction of adiponectin, AdipoR2 and T-cadherin in PyV-mT mammary tumors and raise the possibility of their concerted regulation or interactions in the mammary gland.

Restricted MMTV-PyV-mT Mammary Tumor Growth in Adiponectin Null Mice

To investigate the contributions of adiponectin in mammary tumorigenesis, we introduced the adiponectin null mutation into the syngeneic C57Bl/6 MMTV-PyV-mT transgenic mice and generated homozygous APN-KO and WT female offspring in the second generation. Both WT and APN-KO MMTV-PyV-mT mice developed tumors. Tumor onset was defined as the age of a mouse when the first tumor could be palpated. WT females presented the first tumor at a median age of 73 days while tumors were first detected at 94 days in APN-KO mice (n=17 for WT and n=33 for APN-KO). Thus, tumor onset was delayed by an average of 21 days in APN-KO mice compared to WT controls (Fig. 2A).

To probe if adiponectin affected early tumor development, we investigated MMTV-PyV-mT-induced neoplasias in number 4 mammary gland whole mount preparations from WT and APN-KO mice. At 84 days of age, we registered a 2.2-fold reduction in neoplastic area in APN-KO animals (5.41 ± 0.94%) compared to WT controls (11.73 ± 1.72%) (Fig. 2B). The reduction of neoplastic growth at early stages is in line with the later occurrence of mammary tumors in the APN-KO mice.

Impaired tumor growth in APN-KO MMTV-PyV-mT transgenic mice extended life span. While WT PyV-mT mice survived for an average of 130 days, tumor-bearing APN-KO mice carried on for a median of 160 days (Fig. 2C; n=17 for WT and n=33 for APN-KO). The institutionally determined experimental endpoint was when the largest tumor reached the maximal size of 20 mm over one axis or when animal became moribund. The extended survival rates of APN-KO mice reflect the retardation in tumor onset and a possible reduction in the tumor growth kinetics. Indeed, linear regression analysis of tumor growth in APN-KO and WT MMTV-PyV-mT mice revealed significantly reduced growth rates of APN-KO versus WT tumors (Fig. 2D). In combination, these data show that loss of adiponectin leads to delayed onset and slower growth of mammary tumors and increased survival of affected animals.

Limited Vascularization in Adiponectin-deficient MMTV-PyV-mT Tumors

Pathological analysis of WT and APN-KO tumors revealed presence of solid or papillary adenocarcinomas and adenosquamous carcinomas without clear histological differences between genotypes. This suggests that the pathology of APN-KO tumors remained within the normal range of MMTV-PyV-mT tumors (31). Tumor growth depends on sufficient oxygen and nutrient supply through blood vessels. To determine if adiponectin affects tumor angiogenesis, we examined vascular coverage of APN-KO and WT PyV-mT tumors. Vessel density as determined by CD31 immunostaining was reduced by 47% in APN-KO tumors versus WT (WT, 5.81 ± 0.83% versus APN-KO, 3.09 ± 0.54%, $p < 0.01$, Fig. 3A; n=34 tumors

for WT and n=35 tumors for APN-KO). These data suggest an angiogenic contribution of adiponectin to tumorigenesis.

To gain further insight into the cellular alterations of APN-KO mammary tumors, we examined the degree of hypoxia and apoptotic cell death in tumors from both genotypes. Hypoxyprobe identified 39.86 ± 5.59% of the total APN-KO tumor area as hypoxic versus 28.08 ± 1.97% in WT tumors ($p < 0.05$). This reflects a 42% increase of hypoxic tissue in APN-KO over WT tumors (Fig. 3B). Furthermore, TUNEL staining indicated a 2.4-fold significant increase of apoptotic cells in APN-KO tumors versus controls (WT, 1.6 ± 0.23% versus APN-KO, 3.85 ± 1.02%, $p < 0.05$, Fig. 3C). Proliferation rates as measured by counting PCNA-positive nuclei showed no statistically significant difference between genotypes, although a trend towards reduced proliferation in APN-KO animals was noted (WT, 13.3 ± 2.01%, n = 5 versus APN-KO, 9.97 ± 1.05%, n = 6, $p > 0.05$, data not shown). These combined data suggest a pro-angiogenic contribution of adiponectin with increased hypoxia and apoptosis in APN-KO mammary tumors.

Increased Metastatic Rates in APN-KO MMTV-PyV-mT Tumors

Tumor cells respond to a hypoxic tumor microenvironment with changes in tumor behavior. Although we could not identify pathological changes in APN-KO tumors versus WT, analyses of right lung serial sections at experimental endpoint (Fig. 3D) revealed an increase in the number of pulmonary metastases in the APN-KO condition (6.8 ± 2.08, n=12 animals) versus WT (1.9 ± 0.63, n=10 animals, $p < 0.05$). Since adiponectin is not detected in association with tumor cells in WT mouse MMTV-PyV-mT tumors, we attribute the higher metastatic rates in the APN-KO to the limitation of tumor angiogenesis that leads to hypoxia and in turn supports a metastatic phenotype.

High Molecular Weight Adiponectin Induces Angiogenesis in the Cornea

Adiponectin is prominently present in the serum as the high-molecular-weight (HMW) isoform (32). HMW adiponectin binds T-cadherin and is suggested to be the physiologically most relevant isoform (33). To test if HMW-APN is sufficient to induce angiogenesis, we tested HMW-adiponectin-induced angiogenesis into the normally avascular cornea of WT mice. Slow-release pellets containing eukaryotically produced, recombinant HMW adiponectin (500 ng), vascular endothelial growth factor (VEGF; 180 ng) or phosphate-buffered saline (PBS) were implanted close to the center of the cornea. Blood vessel growth towards the implants was monitored on a daily basis. Ten days after surgery, we observed a comparable degree of blood vessel growth towards the VEGF- and adiponectin-implants while no vascularization was detected in the negative controls (Fig. 4). Quantification of angiogenic areas from at least 4 mice in each condition established that supply of HMW-adiponectin in the vicinity of blood vessels is sufficient to induce angiogenesis. These data provide evidence in support the suggestion that adiponectin in the tumor microenvironment contributes to tumor vascularization.

Discussion

Tumor growth and progression are regulated by both intrinsic factors and interactions with the stromal microenvironment. By generating and analyzing an adiponectin null mouse genetic model of mammary cancer, we provide evidence for a proangiogenic contribution of adiponectin to tumor vascularization that in turn promotes tumor growth. Adiponectin strongly associates with the vasculature in both the normal and the tumorigenic mouse and human mammary gland colocalizing with vascular T-cadherin [Fig. 1; Supplementary Fig. 1; (26)]. Loss of adiponectin from the tumor vasculature restricts vessel density thereby limiting oxygen and nutrient supply. PyV-mT tumors are critically dependent on angiogenesis as PyV-mT-

driven tumors expressing MMTV-controlled vascular endothelial growth factor (VEGF) show significantly earlier tumor onset than their wild type counterparts [(34) and personal communication Dr. R.G. Oshima]. Vice versa, limited vascularization as observed in T-cadherin-deficient mice retards tumor growth (26). Thus, vascular starvation of the tumors in APN-KO mice seems a major cause for tumor growth retardation and extension of animal survival.

Functions for adiponectin in vascular cells are well established *in vitro* and *in vivo*: adiponectin promotes endothelial cell migration and differentiation into tube-like structures *in vitro* (11), and *in vivo* accelerates neovascularization after hind limb ischemia (12). We demonstrate here in the corneal assay that the major HMW-adiponectin isoform is physiologically active and sufficient to stimulate angiogenesis similar to VEGF alone (Figure 4). Adiponectin binding to endothelial cells *in vitro* activates downstream signal transduction cascades involving adenosine monophosphate-activated protein kinase (AMPK) (11). The specific membrane receptors and associated signaling intermediates in the vasculature, however, remain to be elucidated. Two seven-span adiponectin receptors, AdipoR1 and AdipoR2 (30) and the GPI-anchored cadherin-type adiponectin-binding protein T-cadherin (35) serve in associating adiponectin with the cellular plasma membrane (33,36).

We note striking parallels of the APN-KO tumor phenotype with the T-cadherin null MMTV-PyV-mT model (26). T-cadherin is sufficient to bind adiponectin (33) and is required for the vascular association of adiponectin in mammary tumors (26). In T-cadherin null mice, loss of vascular adiponectin association dramatically increases adiponectin levels in the circulation (26) implicating a critical role for T-cadherin in adiponectin's cellular association. One possibility is that GPI-linked T-cadherin is part of an oligomeric protein complex that in combination with AdipoRs serves in adiponectin-binding and signaling. The coincident reduction of T-cadherin and AdipoR2 in MMTV-PyV-mT tumors (Figure 1) is consistent with this suggestion. Alternatively, T-cadherin may be necessary for docking circulating adiponectin to the vasculature, thereby regulating its availability to other vascular receptors that in turn activate associated down-stream signaling cascades. Although evidence for the direct mechanistic link between adiponectin and T-cadherin *in vivo* is still lacking, the combined analyses of adiponectin-deficient and T-cadherin-deficient MMTV-PyV-mT mouse models yield strong parallels supporting concerted roles in mammary tumor angiogenesis.

Despite the reduced overall tumor burden and the prolonged life span of APN-KO PyV-mT transgenic mice, autopsies at experimental endpoint show increased metastatic spreading compared to controls (Fig. 2C and 3D). One possible interpretation of this result is that pulmonary metastases increase at the same rate in both WT and APN-KO mice but frequency is enhanced in the KO condition due to longer animal survival. An alternative explanation is that the challenging tumor microenvironment supports an aggressive and lethal tumor phenotype after a honeymoon phase of disease improvement. Indeed, multiple *in vitro* studies have linked hypoxia to increased tumor cell invasiveness (37-39). Moreover, MMTV-PyV-mT-tumors lacking Hypoxia-Inducible Factor-α (HIF-1α) display reduced pulmonary metastases (40). In APN-KO mice, PyV-mT mammary tumors show significantly larger hypoxic areas than in WT animals thus linking enhanced hypoxic signaling to increased pulmonary metastases. These observations relate to clinical findings that drug inhibitors of the pro-angiogenic VEGF pathway typically lead to only temporary improvements, and breast cancers resist such treatment after a limited time frame (41). The identification of the alternative adiponectin-induced pro-angiogenic pathway reported here might open new opportunities for drug development that may help overcome this limitation.

MMTV-PyV-mT transgenic mice reliably represent ErbB2-overexpressing human breast cancer. Numerous studies have demonstrated that MMTV-PyV-mT-induced tumors mimic

human ErbB2 carcinomas in terms of biomarker expression, stages of tumor progression, distant metastases and activation of down-stream signaling pathways (15-25). We detect adiponectin solely in association with the tumor vasculature in both the mouse model and in human mammary carcinomas implicating tumor blood vessels as primary adiponectin targets. The current mouse genetic model consistently identifies a prominent pro-angiogenic contribution of adiponectin in tumorigenesis. Epidemiological studies have implicated a tumor protective role of adiponectin in humans (6,7). The PyV-mT mouse mammary tumor model, however, does not support a cancer protective function. The current study provides clear evidence for a novel and unexpected contribution of adiponectin to tumor angiogenesis. Future work will need to address if adiponectin exerts dual functions in tumors that may weigh differently depending on the tumor type. It will also remain an important task to identify changes in the cellular interactions between tumor cells and the stromal microenvironment in relation to serum adiponectin levels. The multiple contributions of adiponectin in cancer and metabolic disease certainly warrant the detailed understanding of the cellular and molecular underpinnings regulating these functions.

Supplementary Material

Refer to Web version on PubMed Central for supplementary material.

Acknowledgments

We thank Dr. Robert Oshima (Burnham Institute for Medical Research, La Jolla) for helpful discussions and suggestions throughout this work and comments on the manuscript. We gratefully acknowledge Dr. Norikazu Maeda, Dr. Tohru Funahashi and Dr. Yuji Matsuzawa (Osaka University, Japan) for generating and generously providing the APN-KO mice. Dr. Simone Codeluppi (Burnham Institute for Medical Research, La Jolla) gave advice on the statistical analyses, and Dr. Stan Krajewski (Burnham Institute for Medical Research, La Jolla) assisted with the algorithms for histological tumor analysis. Ms. Adriana Charbono of the Burnham Institute's Animal Facility and Ms. Robbin Newlin, Ms. Karen Teofilo and Mr. Ronald Torres of the Burnham Institute's Histology/Molecular Pathology Facility contributed outstanding technical support to this work.

Grant support: NIH Grant HD25938 (B. Ranscht), National Cancer Institute grant CA 098778 (R.D. Cardiff), Boehringer Ingelheim Fonds (M.S. Denzel).

References

1. Joyce JA. Therapeutic targeting of the tumor microenvironment. Cancer Cell 2005;7:513–20. [PubMed: 15950901]
2. Chen MP, Tsai JC, Chung FM, et al. Hypoadiponectinemia is associated with ischemic cerebrovascular disease. Arterioscler Thromb Vasc Biol 2005;25:821–6. [PubMed: 15692106]
3. Hotta K, Funahashi T, Arita Y, et al. Plasma concentrations of a novel, adipose-specific protein, adiponectin, in type 2 diabetic patients. Arterioscler Thromb Vasc Biol 2000;20:1595–9. [PubMed: 10845877]
4. Iwashima Y, Katsuya T, Ishikawa K, et al. Hypoadiponectinemia is an independent risk factor for hypertension. Hypertension 2004;43:1318–23. [PubMed: 15123570]
5. Kumada M, Kihara S, Sumitsuji S, et al. Association of hypoadiponectinemia with coronary artery disease in men. Arterioscler Thromb Vasc Biol 2003;23:85–9. [PubMed: 12524229]
6. Chen DC, Chung YF, Yeh YT, et al. Serum adiponectin and leptin levels in Taiwanese breast cancer patients. Cancer Lett 2006;237:109–14. [PubMed: 16019138]
7. Mantzoros C, Petridou E, Dessypris N, et al. Adiponectin and breast cancer risk. J Clin Endocrinol Metab 2004;89:1102–7. [PubMed: 15001594]
8. Kang JH, Yu BY, Youn DS. Relationship of serum adiponectin and resistin levels with breast cancer risk. J Korean Med Sci 2007;22:117–21. [PubMed: 17297263]

9. Wang Y, Lam JB, Lam KS, et al. Adiponectin modulates the glycogen synthase kinase-3beta/beta-catenin signaling pathway and attenuates mammary tumorigenesis of MDA-MB-231 cells in nude mice. Cancer Res 2006;66:11462–70. [PubMed: 17145894]
10. Folkman J. Tumor angiogenesis. Adv Cancer Res 1985;43:175–203. [PubMed: 2581424]
11. Ouchi N, Kobayashi H, Kihara S, et al. Adiponectin stimulates angiogenesis by promoting cross-talk between AMP-activated protein kinase and Akt signaling in endothelial cells. J Biol Chem 2004;279:1304–9. [PubMed: 14557259]
12. Shibata R, Ouchi N, Kihara S, Sato K, Funahashi T, Walsh K. Adiponectin stimulates angiogenesis in response to tissue ischemia through stimulation of amp-activated protein kinase signaling. J Biol Chem 2004;279:28670–4. [PubMed: 15123726]
13. Maeda N, Shimomura I, Kishida K, et al. Diet-induced insulin resistance in mice lacking adiponectin/ACRP30. Nat Med 2002;8:731–7. [PubMed: 12068289]
14. Slamon DJ, Clark GM, Wong SG, Levin WJ, Ullrich A, McGuire WL. Human breast cancer: correlation of relapse and survival with amplification of the HER-2/neu oncogene. Science 1987;235:177–82. [PubMed: 3798106]
15. Dilworth SM. Polyoma virus middle T antigen and its role in identifying cancer-related molecules. Nat Rev Cancer 2002;2:951–6. [PubMed: 12459733]
16. Herschkowitz JI, Simin K, Weigman VJ, et al. Identification of conserved gene expression features between murine mammary carcinoma models and human breast tumors. Genome Biol 2007;8:R76. [PubMed: 17493263]
17. Lin EY, Jones JG, Li P, et al. Progression to malignancy in the polyoma middle T oncoprotein mouse breast cancer model provides a reliable model for human diseases. Am J Pathol 2003;163:2113–26. [PubMed: 14578209]
18. Kouros-Mehr H, Bechis SK, Slorach EM, et al. GATA-3 links tumor differentiation and dissemination in a luminal breast cancer model. Cancer Cell 2008;13:141–52. [PubMed: 18242514]
19. Kouros-Mehr H, Kim JW, Bechis SK, Werb Z. GATA-3 and the regulation of the mammary luminal cell fate. Curr Opin Cell Biol 2008;20:164–70. [PubMed: 18358709]
20. Kouros-Mehr H, Slorach EM, Sternlicht MD, Werb Z. GATA-3 maintains the differentiation of the luminal cell fate in the mammary gland. Cell 2006;127:1041–55. [PubMed: 17129787]
21. Brison O. Gene amplification and tumor progression. Biochim Biophys Acta 1993;1155:25–41. [PubMed: 8504129]
22. Menard S, Tagliabue E, Campiglio M, Pupa SM. Role of HER2 gene overexpression in breast carcinoma. J Cell Physiol 2000;182:150–62. [PubMed: 10623878]
23. Lapidus RG, Nass SJ, Davidson NE. The loss of estrogen and progesterone receptor gene expression in human breast cancer. J Mammary Gland Biol Neoplasia 1998;3:85–94. [PubMed: 10819507]
24. Namba R, Young LJ, Maglione JE, et al. Selective estrogen receptor modulators inhibit growth and progression of premalignant lesions in a mouse model of ductal carcinoma in situ. Breast Cancer Res 2005;7:R881–9. [PubMed: 16280035]
25. Guy CT, Cardiff RD, Muller WJ. Induction of mammary tumors by expression of polyomavirus middle T oncogene: a transgenic mouse model for metastatic disease. Mol Cell Biol 1992;12:954–61. [PubMed: 1312220]
26. Hebbard LW, Garlatti M, Young LJ, Cardiff RD, Oshima RG, Ranscht B. T-cadherin supports angiogenesis and adiponectin association with the vasculature in a mouse mammary tumor model. Cancer Res 2008;68:1407–16. [PubMed: 18316604]
27. Mulrane L, Rexhepaj E, Smart V, et al. Creation of a digital slide and tissue microarray resource from a multi-institutional predictive toxicology study in the rat: an initial report from the PredTox group. Exp Toxicol Pathol 2008;60:235–45. [PubMed: 18479893]
28. Kenyon BM, Browne F, D'Amato RJ. Effects of thalidomide and related metabolites in a mouse corneal model of neovascularization. Exp Eye Res 1997;64:971–8. [PubMed: 9301478]
29. Berg AH, Combs TP, Du X, Brownlee M, Scherer PE. The adipocyte-secreted protein Acrp30 enhances hepatic insulin action. Nat Med 2001;7:947–53. [PubMed: 11479628]
30. Yamauchi T, Kamon J, Ito Y, et al. Cloning of adiponectin receptors that mediate antidiabetic metabolic effects. Nature 2003;423:762–9. [PubMed: 12802337]

31. Ellies LG, Fishman M, Hardison J, et al. Mammary tumor latency is increased in mice lacking the inducible nitric oxide synthase. Int J Cancer 2003;106:1–7. [PubMed: 12794750]
32. Shibata R, Ouchi N, Ito M, et al. Adiponectin-mediated modulation of hypertrophic signals in the heart. Nat Med 2004;10:1384–9. [PubMed: 15558058]
33. Hug C, Wang J, Ahmad NS, Bogan JS, Tsao TS, Lodish HF. T-cadherin is a receptor for hexameric and high-molecular-weight forms of Acrp30/adiponectin. Proc Natl Acad Sci U S A 2004;101:10308–13. [PubMed: 15210937]
34. Oshima RG, Lesperance J, Munoz V, et al. Angiogenic acceleration of Neu induced mammary tumor progression and metastasis. Cancer Res 2004;64:169–79. [PubMed: 14729621]
35. Ranscht B, Dours-Zimmermann MT. T-cadherin, a novel cadherin cell adhesion molecule in the nervous system lacks the conserved cytoplasmic region. Neuron 1991;7:391–402. [PubMed: 1654948]
36. Kadowaki T, Yamauchi T. Adiponectin and adiponectin receptors. Endocr Rev 2005;26:439–51. [PubMed: 15897298]
37. Graham CH, Forsdike J, Fitzgerald CJ, Macdonald-Goodfellow S. Hypoxia-mediated stimulation of carcinoma cell invasiveness via upregulation of urokinase receptor expression. Int J Cancer 1999;80:617–23. [PubMed: 9935166]
38. Krishnamachary B, Berg-Dixon S, Kelly B, et al. Regulation of colon carcinoma cell invasion by hypoxia-inducible factor 1. Cancer Res 2003;63:1138–43. [PubMed: 12615733]
39. Munoz-Najar UM, Neurath KM, Vumbaca F, Claffey KP. Hypoxia stimulates breast carcinoma cell invasion through MT1-MMP and MMP-2 activation. Oncogene 2006;25:2379–92. [PubMed: 16369494]
40. Liao D, Corle C, Seagroves TN, Johnson RS. Hypoxia-inducible factor-1alpha is a key regulator of metastasis in a transgenic model of cancer initiation and progression. Cancer Res 2007;67:563–72. [PubMed: 17234764]
41. Bergers G, Hanahan D. Modes of resistance to anti-angiogenic therapy. Nat Rev Cancer 2008;8:592–603. [PubMed: 18650835]

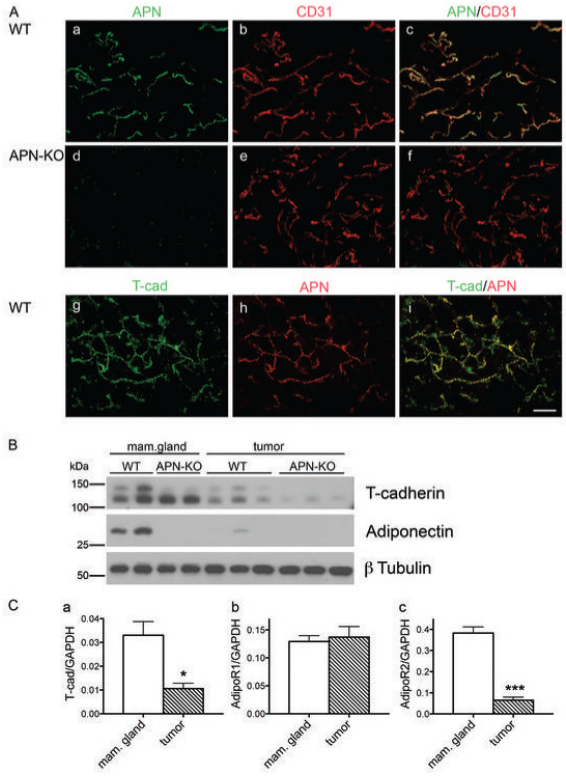

Figure 1. Adiponectin in the mammary gland

A, Adiponectin delineates the vasculature and colocalizes with the adiponectin-binding protein T-cadherin. Immunostaining of normal mammary fat pads from virgin WT (a, b, c, g, h, i) and APN-KO (d, e, f) mice for adiponectin (a, d, h), CD31 (b, e) and T-cadherin (g). Merged confocal images (c, f, i) identify adiponectin in the WT vasculature and reveals absence of adiponectin in the KO condition. In the WT, adiponectin colocalizes with T-cadherin (g, h, i). Bar, 50 μm.

B, Adiponectin levels are reduced in MMTV-PyV-mT tumors. Immunoblot from virgin mammary gland and MMTV-PyV-mT-induced mammary tumors from WT and APN-KO mice. T-cadherin migrates as a proportein of 130 kDa and a mature protein of 105 kDa. Tumors display reduced T-cadherin levels coincident with the reduction in adiponectin in tumor tissue.

C, T-cadherin and AdipoR2 expression levels are significantly reduced in tumors. Real-time quantitative PCR for T-cadherin (a), AdipoR1 (b) and AdipoR2 (c) mRNA in normal breast (n = 3) and tumor tissue (n = 3) (unpaired t test).

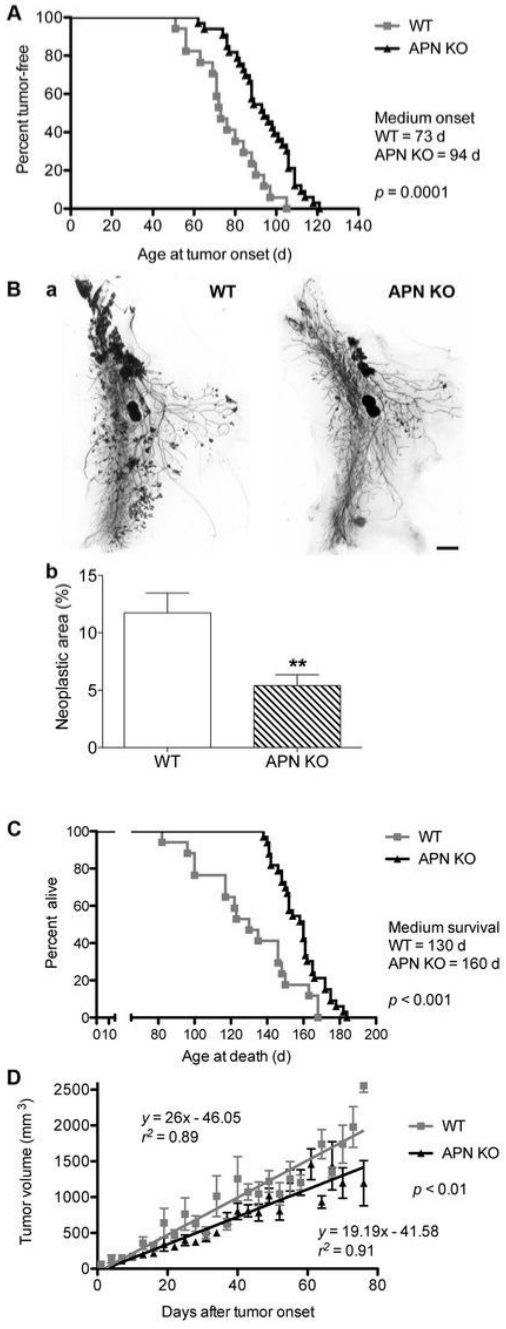

Figure 2. Adiponectin-deficient mice display limited tumor growth

A, Age at tumor onset. Medium age at first detection of MMTV-PyV-MT-induced tumors was 73 days in WT (n = 17 mice) and 94 days in APN-KO mice (n = 33 mice; log-rank test: statistically significant).

B, Carmine-stained whole mount preparations of number 4 mammary glands at 84 days of age (a) and quantification (b) of neoplastic area reveals a reduction of neoplastic area in the APN-KO versus WT mice (WT, n=22; APN-KO, n = 19; statistically significant by unpaired t test, **p < 0.01). Bar, 2 mm.

C, Extended survival rates of APN-KO compared to WT MMTV-PyV-MT-transgenic animals. Median survival is 130 days in the WT (n=17) and 160 days in APN-KO animals (n=33). Log-rank test shows statistical significance.

D, Tumor volume as a function of time after first tumor appearance. Linear regression analysis shows a statistically significant reduction in the growth kinetics of the largest two tumors in APN-KO mice (n = 33) versus WT (n = 17) mice.

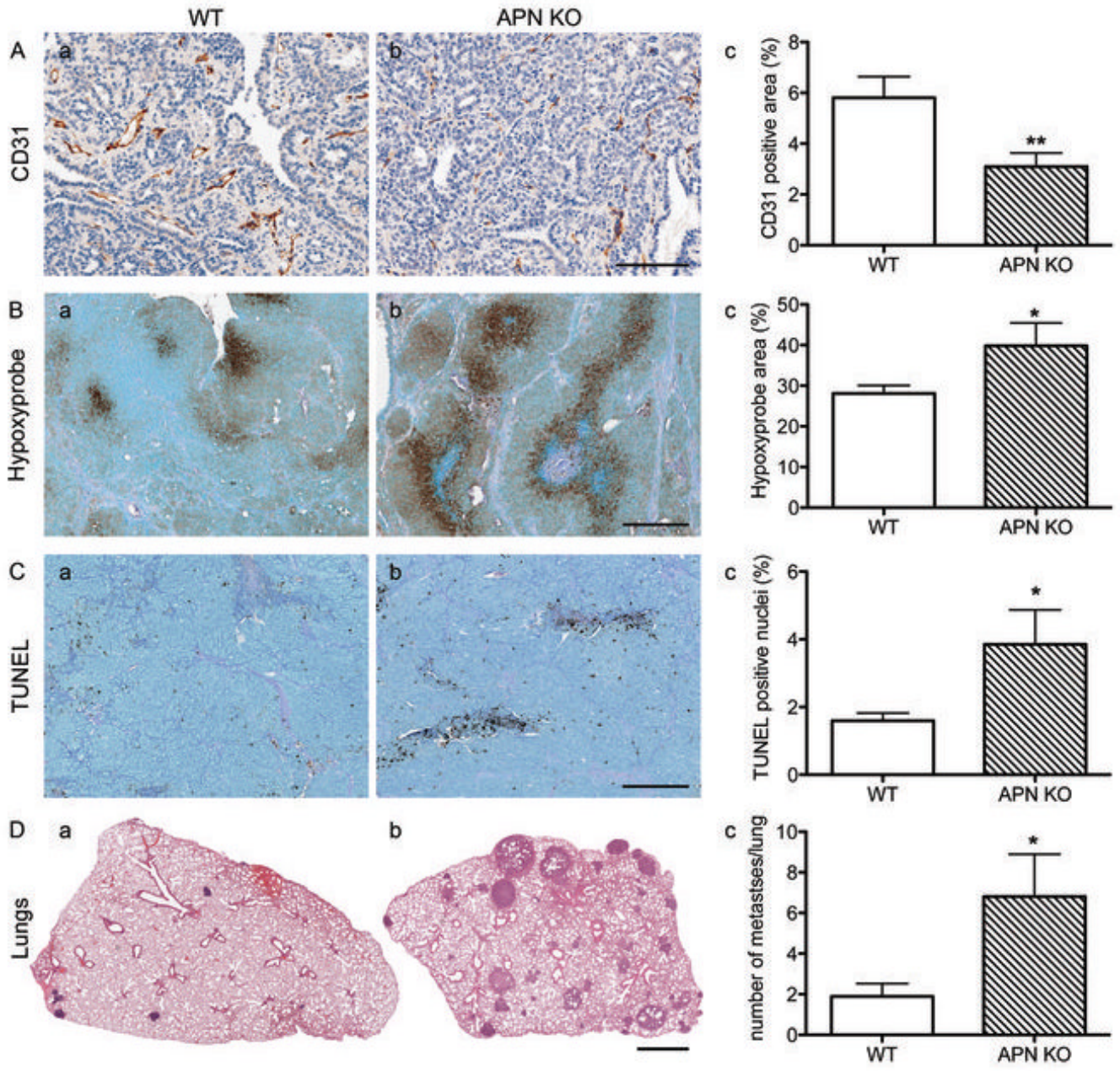

Figure 3. APN-KO tumors display low vascular density, increased hypoxia, elevated apoptosis, and increased metastases compared to the WT

A, Quantification of CD31-positive area of complete tumor sections from WT (a) and APN-KO mice (b) shows a statistically significant reduction in APN-KO mice (c) (WT, n=34; APN-KO, n=35 tumors; *$p < 0.01$, unpaired t-test). Bar, 100 μm.

B, Detection of hypoxic areas in tumors with Hypoxyprobe reveals increases in APN-KO tumors (b) over tumors from WT controls (a). Total hypoxia is significantly elevated in APN-KO tumors (c; WT, n=9; APN-KO, n=4 tumors; *$p < 0.05$). Bar, 200 μm.

C, Analysis of TUNEL-positive nuclei from WT (a, n=30) and APN-KO tumors (b, n=31; *$p < 0.05$ by unpaired t-test) reveals a statistically significant increase of apoptotic cells. Bar, 200 μm.

D, Representative H&E-stained lung cross-sections of tumor bearing WT (a) and APN-KO (b) animals show increased metastases in APN-KO mice (n=12 animals) compared to the WT (c, n=10 animals, *$p < 0.05$ by Mann-Whitney test). Bar, 1 mm.

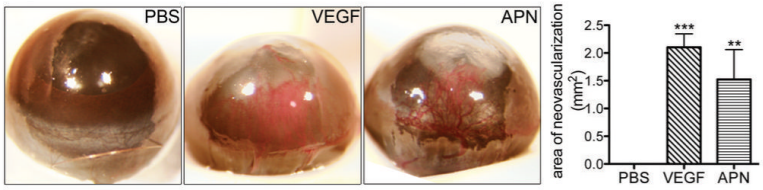

Figure 4. Adiponectin induces angiogenesis in the corneal micropocket assay

Photomicrographs of adult mouse eyes 10 days after implantation of Hydron pellets containing PBS (n=6), 180 ng VEGF (n=5), or 500 ng high-molecular-weight adiponectin (n=4). Adiponectin significantly induces corneal angiogenesis (one-way ANOVA).